

**$\pi K$  scattering in full QCD with domain-wall valence quarks**Silas R. Beane,<sup>1</sup> Paulo F. Bedaque,<sup>2</sup> Thomas C. Luu,<sup>3</sup> Kostas Orginos,<sup>4,5</sup> Elisabetta Pallante,<sup>6</sup> Assumpta Parreño,<sup>7</sup> and Martin J. Savage<sup>8</sup>

(NPLQCD Collaboration)

<sup>1</sup>*Department of Physics, University of New Hampshire, Durham, New Hampshire 03824-3568, USA*<sup>2</sup>*Department of Physics, University of Maryland, College Park, Maryland 20742-4111, USA*<sup>3</sup>*N Division, Lawrence Livermore National Laboratory, Livermore, California 94551, USA*<sup>4</sup>*Department of Physics, College of William and Mary, Williamsburg, Virginia 23187-8795, USA*<sup>5</sup>*Jefferson Laboratory, 12000 Jefferson Avenue, Newport News, Virginia 23606, USA*<sup>6</sup>*Institute for Theoretical Physics, University of Groningen, Nijenborgh 4, 9747 AG Groningen, The Netherlands*<sup>7</sup>*Departament d'Estructura i Constituents de la Matèria, Universitat de Barcelona, E-08028 Barcelona, Spain*<sup>8</sup>*Department of Physics, University of Washington, Seattle, Washington 98195-1560, USA*

(Received 17 August 2006; published 8 December 2006)

We calculate the  $\pi^+ K^+$  scattering length in fully-dynamical lattice QCD with domain-wall valence quarks on MILC lattices with rooted staggered sea-quarks at a lattice spacing of  $b = 0.125$  fm, lattice spatial size of  $L = 2.5$  fm and at pion masses of  $m_\pi \sim 290, 350, 490$  and  $600$  MeV. The lattice data, analyzed at next-to-leading order in chiral perturbation theory, allows an extraction of the full  $\pi K$  scattering amplitude at threshold. Extrapolating to the physical point gives  $m_\pi a_{3/2} = -0.0574 \pm 0.0016^{+0.0024}_{-0.0058}$  and  $m_\pi a_{1/2} = 0.1725 \pm 0.0017^{+0.0023}_{-0.0156}$  for the  $I = 3/2$  and  $I = 1/2$  scattering lengths, respectively, where the first error is statistical and the second error is an estimate of the systematic due to truncation of the chiral expansion.

DOI: [10.1103/PhysRevD.74.114503](https://doi.org/10.1103/PhysRevD.74.114503)

PACS numbers: 12.38.Gc

**I. INTRODUCTION**

In hadronic atoms, nature has provided a relatively clean environment in which to explore the low-energy interactions of charged hadrons. The electromagnetic interaction allows for oppositely-charged, long-lived hadrons to form Coulomb bound states. The locations of the energy levels of these systems are perturbed by the strong interactions, while the lifetimes of the ground states are dictated by the strong interactions that couple the charged hadrons to lighter neutral ones.

Theoretically, the simplest hadronic atom to understand is composed of two pions:  $\pi^+ \pi^-$ . Precision experiments have been performed—and are ongoing—to measure the lifetimes and energy levels of such atoms [1]. In the isospin limit, Bose statistics dictates that two pions interacting in an  $s$ -wave can be in either an isospin-0 or isospin-2 state. By measuring the decay width and energy levels of ponium, the  $I = 0$  and  $I = 2$  strong-interaction scattering lengths can be isolated. While the difference between energy levels, and hence deviations from the Coulomb spectrum, are relatively straightforward to measure, it is somewhat more challenging to determine the lifetime of these atoms. Recently, the DIRAC collaboration [1] at CERN has measured the lifetime to be  $\tau_{\pi^+ \pi^-} = 2.91^{+0.49}_{-0.62} \times 10^{-15}$  s, with the dominant decay mode being  $\pi^+ \pi^- \rightarrow 2\pi^0$ . On the theoretical side, progress in lattice QCD has been quite rapid, with a recent fully-dynamical

calculation of the  $I = 2$   $\pi\pi$  scattering length at pion masses between  $m_\pi \sim 290$  MeV and  $500$  MeV [2]. When combined with two-flavor chiral perturbation theory, a prediction of the scattering length at the physical point is found to have an uncertainty that is somewhat smaller than that from experiment. An up-to-date discussion of the status of  $\pi\pi$ -interactions can be found in Ref. [3].

Studying the low-energy interactions between kaons and pions with  $\pi^- K^+$  bound-states allows for an explicit exploration of the three-flavor structure of low-energy hadronic interactions, an aspect that is not directly probed in  $\pi\pi$  scattering. Experiments have been proposed by the DIRAC collaboration [4] to study  $\pi K$  atoms at CERN, J-PARC and GSI, the results of which would provide direct measurements or constraints on combinations of the scattering lengths. In the isospin limit, there are two isospin channels available to the  $\pi K$  system,  $I = \frac{1}{2}$  and  $I = \frac{3}{2}$ . The width of a  $\pi^- K^+$  atom depends upon the difference between scattering lengths in the two channels,  $\Gamma \sim (a_{1/2} - a_{3/2})^2$ , (where  $a_{1/2}$  and  $a_{3/2}$  are the  $I = \frac{1}{2}$  and  $I = \frac{3}{2}$  scattering lengths, respectively) while the shift of the ground state depends upon a different combination,  $\Delta E_0 \sim 2a_{1/2} + a_{3/2}$ . Recently, the Roy-Steiner equations (analyticity, unitarity and crossing-symmetry) have been used to extrapolate high-energy  $\pi K$  data down to threshold [5], where it is found that

$$\begin{aligned} m_\pi(a_{1/2} - a_{3/2}) &= 0.269 \pm 0.015, \\ m_\pi(a_{1/2} + 2a_{3/2}) &= 0.134 \pm 0.037, \end{aligned} \quad (1)$$

which can be decomposed to  $m_\pi a_{1/2} = 0.224 \pm 0.022$  and  $m_\pi a_{3/2} = -0.0448 \pm 0.0077$ . (See also Ref. [6] for a similar approach.) In addition, three-flavor chiral perturbation theory ( $\chi$ PT) has been used to predict these scattering lengths out to next-to-next-to-leading order (NNLO) in the chiral expansion. At NLO [7–9],

$$\begin{aligned} m_\pi(a_{1/2} - a_{3/2}) &= 0.238 \pm 0.002, \\ m_\pi(a_{1/2} + 2a_{3/2}) &= 0.097 \pm 0.047, \end{aligned} \quad (2)$$

while at NNLO [10]  $m_\pi a_{1/2} = 0.220$  and  $m_\pi a_{3/2} = -0.047$ .<sup>1</sup> One must be cautious in assessing the uncertainties in these theoretical calculations, as one can only make estimates based on power-counting for the contribution of higher-order terms in the chiral expansion. There has been one determination of the  $\pi^+ K^+$  scattering length in quenched QCD [12], however, the chiral extrapolation of the scattering length did not include the non-analytic dependences on the light-quark masses that are predicted by chiral perturbation theory.

It is worth mentioning a novel motivation for accurate determinations of meson-meson scattering from lattice QCD calculations. Recent work has identified in a model-independent way the lowest-lying resonance in QCD which appears in  $\pi\pi$  scattering [13]. Crucial to this development has been the accurate determination of the low-energy  $\pi\pi$  scattering amplitude, including the recent lattice QCD determination of the  $I = 2$  scattering length [2]. A similar analysis has very recently been carried out for  $\pi K$  scattering in the  $I = \frac{1}{2}$   $s$ -wave in order to determine the lowest-lying strange resonance [14]. Improved accuracy in the low-energy  $\pi K$  scattering amplitude should be welcome to this endeavor.

In this work we present the results of a fully-dynamical lattice QCD calculation of  $\pi^+ K^+$  scattering. By calculating the  $m_\pi$  and  $m_K$  dependence of the  $\pi^+ K^+$  ( $I = \frac{3}{2}$ ) scattering length, we are able to provide a determination of both the  $I = \frac{3}{2}$  and  $I = \frac{1}{2}$  scattering lengths at the physical point. We have performed a hybrid mixed-action calculation with domain-wall valence quarks tuned to the staggered sea-quark masses of the MILC configurations. As the computer resources do not presently exist to perform such calculations at or very near the physical value of the light-quark masses, these are performed at pion masses between  $m_\pi \sim 290$  MeV and  $\sim 600$  MeV. These results are combined with calculations in continuum three-flavor  $\chi$ PT to extrapolate to the physical point.

<sup>1</sup>At tree level, Weinberg [11] determined that  $m_\pi a_{1/2} = 0.137$  and  $m_\pi a_{3/2} = -0.0687$ .

## II. FINITE-VOLUME CALCULATION OF SCATTERING AMPLITUDES

The  $s$ -wave scattering amplitude for two particles below inelastic thresholds can be determined using Lüscher’s method [15], which entails a measurement of one or more energy levels of the two-particle system in a finite volume. For two particles with masses  $m_1$  and  $m_2$  in an  $s$ -wave, with zero total three momentum, and in a finite volume, the difference between the energy levels and those of two noninteracting particles can be related to the inverse scattering amplitude via the eigenvalue equation [15]

$$p \cot \delta(p) = \frac{1}{\pi L} \mathbf{S}\left(\frac{pL}{2\pi}\right), \quad (3)$$

where  $\delta(p)$  is the elastic-scattering phase shift, and the regulated three-dimensional sum is

$$\mathbf{S}(\eta) \equiv \sum_{\mathbf{j}}^{|j| < \Lambda} \frac{1}{|\mathbf{j}|^2 - \eta^2} - 4\pi\Lambda. \quad (4)$$

The sum in Eq. (4) is over all triplets of integers  $\mathbf{j}$  such that  $|\mathbf{j}| < \Lambda$  and the limit  $\Lambda \rightarrow \infty$  is implicit [16]. This definition is equivalent to the analytic continuation of zeta-functions presented by Lüscher [15]. In Eq. (3),  $L$  is the length of the spatial dimension in a cubically-symmetric lattice. The energy eigenvalue  $E_n$  and its deviation from the sum of the rest masses of the particle,  $\Delta E_n$ , are related to the center-of-mass momentum  $p_n$ , a solution of Eq. (3), by

$$\begin{aligned} \Delta E_n &\equiv E_n - m_1 - m_2 \\ &= \sqrt{p_n^2 + m_1^2} + \sqrt{p_n^2 + m_2^2} - m_1 - m_2 \\ &= \frac{p_n^2}{2\mu_{12}} + \dots, \end{aligned} \quad (5)$$

where  $\mu_{12}$  is the reduced mass of the system. In the absence of interactions between the particles,  $|p \cot \delta| = \infty$ , and the energy levels occur at momenta  $\mathbf{p} = 2\pi\mathbf{j}/L$ , corresponding to single-particle modes in a cubic cavity. Expanding Eq. (3) about zero momenta,  $p \sim 0$ , one obtains the familiar relation<sup>2</sup>

$$\Delta E_0 = -\frac{2\pi a}{\mu_{12} L^3} \left[ 1 + c_1 \frac{a}{L} + c_2 \left(\frac{a}{L}\right)^2 \right] + \mathcal{O}\left(\frac{1}{L^6}\right), \quad (6)$$

with

$$\begin{aligned} c_1 &= \frac{1}{\pi} \sum_{\mathbf{j} \neq \mathbf{0}}^{|j| < \Lambda} \frac{1}{|\mathbf{j}|^2} - 4\Lambda = -2.837297, \\ c_2 &= c_1^2 - \frac{1}{\pi^2} \sum_{\mathbf{j} \neq \mathbf{0}} \frac{1}{|\mathbf{j}|^4} = 6.375183, \end{aligned} \quad (7)$$

<sup>2</sup>We have chosen to use the “particle physics” definition of the scattering length, as opposed to the “nuclear physics” definition, which is opposite in sign.

TABLE I. The parameters of the MILC gauge configurations and domain-wall propagators used in this work. The subscript  $l$  denotes light quark (up/down) where  $s$  denotes the strange quark. The superscript  $dwf$  denotes the bare quark mass for the domain-wall fermion propagator calculation. The last column is number of configurations times number of sources per configuration.

Ensemble	$bm_l$	$bm_s$	$bm_l^{dwf}$	$bm_s^{dwf}$	$10^3 \times bm_{\text{res}}^a$	# of propagators
2064f21b676m007m050	0.007	0.050	0.0081	0.081	$1.604 \pm 0.038$	$468 \times 4$
2064f21b676m010m050	0.010	0.050	0.0138	0.081	$1.552 \pm 0.027$	$658 \times 4$
2064f21b679m020m050	0.020	0.050	0.0313	0.081	$1.239 \pm 0.028$	$486 \times 3$
2064f21b681m030m050	0.030	0.050	0.0478	0.081	$0.982 \pm 0.030$	$564 \times 6$

<sup>a</sup>Computed by the LHP collaboration.

and  $a$  is the scattering length, defined by

$$a = \lim_{p \rightarrow 0} \frac{\tan \delta(p)}{p}. \quad (8)$$

For the  $I = \frac{3}{2}$   $\pi K$  scattering length,  $a_{3/2}$ , that we compute in this work, the difference between the exact solution to Eq. (3) and the approximate solution in Eq. (6) is much less than 1%.

### III. DETAILS OF THE LATTICE CALCULATION

Our computation uses the mixed-action lattice QCD scheme developed by LHPC [17,18] which places domain-wall valence quarks from a smeared-source on  $N_f = 2 + 1$  asqtad-improved [19,20] MILC configurations generated with rooted<sup>3</sup> staggered sea quarks [29] that are hypercubic-smeared (HYP-smeared) [30–33]. In the generation of the MILC configurations, the strange-quark mass was fixed near its physical value,  $bm_s = 0.050$ , (where  $b = 0.125$  fm is the lattice spacing) determined by the mass of hadrons containing strange quarks. The two light quarks in the configurations are degenerate (isospin-symmetric). As was shown by LHPC [17,18], HYP-smearing allows for a significant reduction in the residual chiral symmetry breaking at a moderate extent  $L_s = 16$  of the extra dimension and domain-wall height  $M_5 = 1.7$ . Using Dirichlet boundary conditions we reduced the original time extent of 64 down to 32. This allowed us to recycle propagators computed for the nucleon structure function calculations performed by LHPC. For bare domain-wall fermion masses we used the tuned values that match the staggered Goldstone pion to few-percent precision. For details of the matching see Refs. [17,18]. The parameters used in the propagator calculation are summarized in Table I. All propagator calculations were performed using the Chroma software suite [34,35].

As it is the difference in the energy between interacting mesons and noninteracting mesons that provides the scattering amplitude, we computed the one-pion correlation

function  $C_{\pi^+}(t)$ , the one-kaon correlation function  $C_{K^+}(t)$ , and the kaon-pion correlation function  $C_{\pi^+K^+}(p, t)$ , where  $t$  denotes the number of time slices between the hadronic-sink and the hadronic-source, and  $p$  denotes the magnitude of the (equal and opposite) momentum of each meson. The single-pion correlation function is

$$C_{\pi^+}(t) = \sum_{\mathbf{x}} \langle \pi^-(t, \mathbf{x}) \pi^+(0, \mathbf{0}) \rangle, \quad (9)$$

where the summation over  $\mathbf{x}$  corresponds to summing over all the spatial lattice sites, thereby projecting onto the momentum  $\mathbf{p} = \mathbf{0}$  state. The single-kaon correlation function has a similar form. The  $\pi^+K^+$  correlation function that projects onto the  $s$ -wave state in the continuum limit is

$$C_{\pi^+K^+}(p, t) = \sum_{|\mathbf{p}|=p} \sum_{\mathbf{x}, \mathbf{y}} e^{i\mathbf{p} \cdot (\mathbf{x} - \mathbf{y})} \langle \pi^-(t, \mathbf{x}) K^-(t, \mathbf{y}) \times K^+(0, \mathbf{0}) \pi^+(0, \mathbf{0}) \rangle, \quad (10)$$

where, in Eqs. (9) and (10),  $\pi^+(t, \mathbf{x}) = \bar{u}(t, \mathbf{x}) \gamma_5 d(t, \mathbf{x})$  is an interpolating field for the  $\pi^+$ , and  $K^+(t, \mathbf{x}) = \bar{u}(t, \mathbf{x}) \gamma_5 s(t, \mathbf{x})$  is an interpolating field for the  $K^+$ . In the relatively large lattice volumes that we are using, the energy difference between the interacting and noninteracting two-meson states is a small fraction of the total energy, which is dominated by the masses of the mesons. In order to extract this energy difference we formed the ratio of correlation functions,  $G_{\pi^+K^+}(p, t)$ , where

$$G_{\pi^+K^+}(p, t) \equiv \frac{C_{\pi^+K^+}(p, t)}{C_{\pi^+}(t) C_{K^+}(t)} \rightarrow \sum_{n=0}^{\infty} \mathcal{A}_n e^{-\Delta E_n t}, \quad (11)$$

and the arrow becomes an equality in the limit of an infinite number of gauge configurations. In  $G_{\pi^+K^+}(p, t)$ , some of the fluctuations that contribute to both the one- and two-meson correlation functions cancel, thereby improving the quality of the extraction of the energy difference beyond what we are able to achieve from an analysis of the individual correlation functions.

### IV. ANALYSIS AND CHIRAL EXTRAPOLATION

A convenient way to present the data is with “effective scattering length” plots, simple variants of effective mass

<sup>3</sup>For recent discussions of the “legality” of the mixed-action and rooting procedures, see Ref. [21–28].

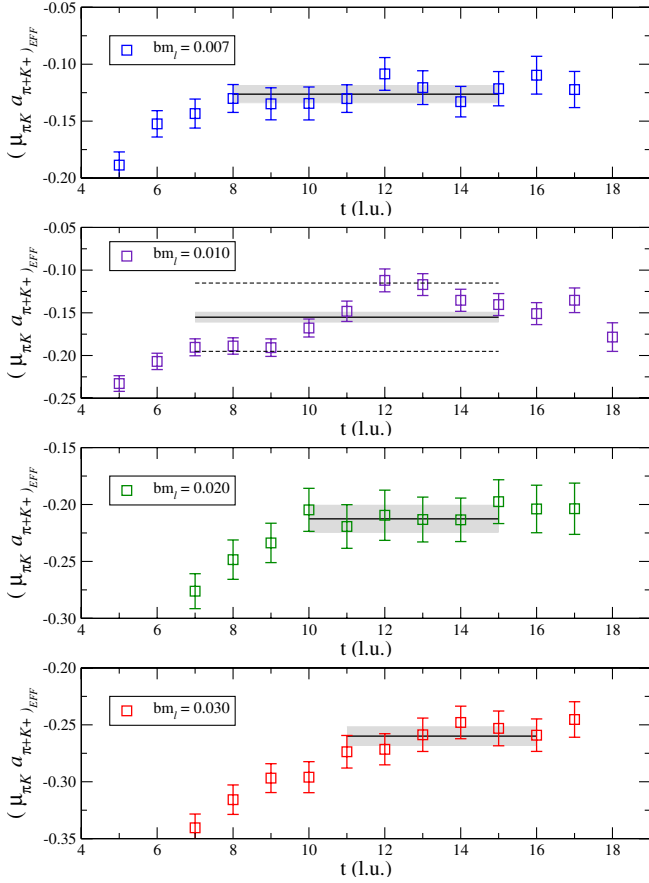


FIG. 1 (color online). The effective  $\pi^+K^+$  scattering length times the reduced mass,  $\mu_{\pi K} a_{\pi^+K^+}(t)$  as a function of time slice arising from smeared sinks. The solid black lines and shaded regions are fits with  $1\text{-}\sigma$  tabulated in Table II. The dashed lines on the m010 ensemble plot are an estimate of a systematic error due to fitting.

plots. The effective energy splitting is formed from the ratio of correlation functions

$$\Delta E_{\pi^+K^+}(t) = \log\left(\frac{G_{\pi^+K^+}(0, t)}{G_{\pi^+K^+}(0, t+1)}\right), \quad (12)$$

which in the limit of an infinite number of gauge configura-

tions would become a constant at large times that is equal to the lowest energy of the interacting kaon and pion in the volume. At each time slice,  $\Delta E_{\pi^+K^+}(t)$  is inserted into Eqs. (3) and (5), or into Eq. (6), to give a scattering length at each time slice,  $a_{\pi^+K^+}(t)$ . It turns out to be more useful to consider the dimensionless quantity of the reduced mass times the scattering length,  $\mu_{\pi K} a_{\pi^+K^+}$ , in our analysis, where  $\mu_{\pi K}(t)$ , the ‘‘effective reduced mass’’ is constructed from the effective mass of the single-particle correlators. For each of the MILC ensembles that we analyze, the effective scattering lengths are shown in Fig. 1. We generated correlators with a point sink and with a smeared sink whose smearing is identical to that of the source. We found that the plateaus in  $\mu_{\pi K} a_{\pi^+K^+}$  are better defined for smeared sinks than those from point sinks.

The energy shifts of the  $\pi^+K^+$  ground state can be extracted directly from the effective scattering length function, or from correlation functions, giving the same results. A single exponential function was fit by  $\chi^2$ -minimization to the correlation functions, from which either the  $\pi^+K^+$  energy or single-particle masses were determined. The central value and uncertainty of each parameter was determined by the jackknife procedure over the ensemble of configurations. The results of our lattice calculation of the decay constants, meson masses,  $\pi^+K^+$  energy shifts and scattering lengths are tabulated in Table II. The scattering lengths as a function of reduced mass are shown in Fig. 2.

As can be seen from Fig. 1, there is a large systematic error associated with the m010 ensemble. There would appear to be two distinct plateaus. Rather than fitting to one of the plateaus, we chose to fit over a large range (7)–(15) which includes both plateaus and then assigned a systematic error which encompasses minima and maxima over the fit range as indicated by the effective scattering length plot. More statistics will have to be acquired on this ensemble before any conclusions can be drawn about this correlator.

In SU(3) chiral perturbation theory [36–38] at NLO, the expansion of the crossing even ( $a^+$ ) and crossing odd ( $a^-$ ) scattering length times the reduced mass is known to be [7–9]

$$\begin{aligned} \mu_{\pi K} a^- &= \frac{\mu_{\pi K}^2}{4\pi f_\pi^2} \left[ 1 + 2 \frac{m_\pi^2}{f_\pi^2} \left[ 8L_5(\lambda) - \frac{1}{16\pi^2} \left\{ \frac{8m_K^2 - 5m_\pi^2}{2(m_K^2 - m_\pi^2)} \log \frac{m_\pi}{\lambda} - \frac{23m_K^2}{9(m_K^2 - m_\pi^2)} \log \frac{m_K}{\lambda} + \frac{28m_K^2 - 9m_\pi^2}{18(m_K^2 - m_\pi^2)} \log \frac{m_\eta}{\lambda} \right. \right. \right. \\ &\quad + \frac{4m_K}{9m_\pi} \frac{\sqrt{(m_K - m_\pi)(2m_K + m_\pi)}}{m_K + m_\pi} \arctan\left(\frac{2(m_K + m_\pi)}{m_K - 2m_\pi} \sqrt{\frac{m_K - m_\pi}{2m_K + m_\pi}}\right) \\ &\quad \left. \left. - \frac{4m_K}{9m_\pi} \frac{\sqrt{(m_K + m_\pi)(2m_K - m_\pi)}}{m_K - m_\pi} \arctan\left(\frac{2(m_K - m_\pi)}{m_K + 2m_\pi} \sqrt{\frac{m_K + m_\pi}{2m_K - m_\pi}}\right) \right] \right], \\ &\equiv \frac{\mu_{\pi K}^2}{4\pi f_\pi^2} \left[ 1 + 16 \frac{m_\pi^2}{f_\pi^2} L_5 + \chi^{(\text{NLO}, -)} \right], \end{aligned} \quad (13)$$

TABLE II. Results from the lattice calculation. All errors are computed from jackknife. The uncertainty associated with the m010 ensemble  $\pi K$  energy shift and related quantities is dominated by the systematic error. The fitting ranges are shown in the square brackets.

Ensemble	$m_\pi/f_\pi$	$m_K/f_\pi$	$\mu_{\pi K}/f_\pi$	$\delta E_{\pi K}$ (MeV)	$\mu_{\pi K} a_{\pi^+ K^+}$	$\Gamma \times 10^3$
m007	2.000(17)	3.980(25)	1.332(10)	11.89(81) [8–15]	-0.1263(75)	-10.1(9)
m010	2.337(11)	3.958(16)	1.469(07)	11.40(50) [7–15]	-0.155(40)	-8(3)
m020	3.059(12)	3.988(15)	1.731(07)	10.15(69) [10–15]	-0.213(12)	-5.59(34)
m030	3.484(10)	4.004(12)	1.869(05)	10.06(54) [11–16]	-0.267(12)	-4.29(15)

$$\begin{aligned} \mu_{\pi K} a^+ &= \frac{\mu_{\pi K}^2 m_K m_\pi}{2\pi f_\pi^4} \left[ 16L_{\pi K}(\lambda) + \frac{1}{16\pi^2} \left\{ \frac{11m_\pi^2}{2(m_K^2 - m_\pi^2)} \log \frac{m_\pi}{\lambda} - \frac{67m_K^2 - 8m_\pi^2}{9(m_K^2 - m_\pi^2)} \log \frac{m_K}{\lambda} + \frac{24m_K^2 - 5m_\pi^2}{18(m_K^2 - m_\pi^2)} \log \frac{m_\eta}{\lambda} \right. \right. \\ &\quad - \frac{4}{9} \frac{\sqrt{(m_K - m_\pi)(2m_K + m_\pi)}}{m_K + m_\pi} \arctan \left( \frac{2(m_K + m_\pi)}{m_K - 2m_\pi} \sqrt{\frac{m_K - m_\pi}{2m_K + m_\pi}} \right) \\ &\quad \left. \left. - \frac{4}{9} \frac{\sqrt{(m_K + m_\pi)(2m_K - m_\pi)}}{m_K - m_\pi} \arctan \left( \frac{2(m_K - m_\pi)}{m_K + 2m_\pi} \sqrt{\frac{m_K + m_\pi}{2m_K - m_\pi}} \right) + \frac{43}{9} \right\} \right], \\ &\equiv \frac{\mu_{\pi K}^2 m_K m_\pi}{2\pi f_\pi^4} [16L_{\pi K} + \chi^{(\text{NLO},+)}] \end{aligned} \quad (14)$$

where the counterterm  $L_{\pi K}(\lambda)$  is a renormalization scale,  $\lambda$ , dependent linear combination of the Gasser-Leutwyler counterterms

$$L_{\pi K} \equiv 2L_1 + 2L_2 + L_3 - 2L_4 - \frac{L_5}{2} + 2L_6 + L_8. \quad (15)$$

It is important to note that the expressions in Eqs. (13) and (14) are written in terms of the full  $f_\pi$ , and not the chiral limit value. The functions  $\chi^{(\text{NLO},+)}(m_\pi/\lambda, m_K/\lambda, m_\eta/\lambda)$  and  $\chi^{(\text{NLO},-)}(m_\pi/\lambda, m_K/\lambda, m_\eta/\lambda)$  clearly depend upon the

renormalization scale  $\lambda$ . In the analysis that follows, it was found to be convenient to normalize the meson masses to  $f_\pi$ , and therefore we can choose the renormalization scale to be  $\lambda = f_\pi^{\text{phys}} = 132$  MeV, and use the values of  $m_\pi/f_\pi$  and  $m_K/f_\pi$  in Table II directly. Deviations between the  $\lambda = f_\pi$  calculated on each lattice and  $\lambda = f_\pi^{\text{phys}}$  are higher order in the chiral expansion.

The  $I = \frac{1}{2}$  and  $I = \frac{3}{2}$  scattering lengths are related to those in Eqs. (13) and (14) by

$$a_{1/2} = a^+ + 2a^- \quad a_{3/2} = a^+ - a^- = a_{\pi^+ K^+}. \quad (16)$$

It is convenient to define the function  $\Gamma$  via a subtraction of the tree-level and one-loop contributions in order to isolate the counterterms,

$$\begin{aligned} \Gamma \left( \frac{m_\pi}{f_\pi}, \frac{m_K}{f_\pi} \right) &\equiv - \frac{f_\pi^2}{16m_\pi^2} \left( \frac{4\pi f_\pi^2}{\mu_{\pi K}^2} [\mu_{\pi K} a_{\pi^+ K^+}] + 1 \right. \\ &\quad \left. + \chi^{(\text{NLO},-)} - 2 \frac{m_K m_\pi}{f_\pi^2} \chi^{(\text{NLO},+)} \right), \end{aligned} \quad (17)$$

where we use the Gell-Mann-Okubo mass-relation among the mesons to determine the  $\eta$ -mass, which we do not measure in this lattice calculation. At NLO this becomes

$$\Gamma = L_5(f_\pi^{\text{phys}}) - 2 \frac{m_K}{m_\pi} L_{\pi K}(f_\pi^{\text{phys}}). \quad (18)$$

It is clear that the dependence of  $\Gamma$  on  $m_\pi$  and  $m_K$  determines  $L_5$  and  $L_{\pi K}$  and, in turn, allows an extraction of  $a_{3/2}$  and  $a_{1/2}$ . The numerical values of  $\Gamma$  and their jackknife errors calculated on each ensemble of lattices are given in Table II, and are plotted in Fig. 3. By fitting a straight line to the values of  $\Gamma$  as a function of  $m_k/m_\pi$  the counterterms

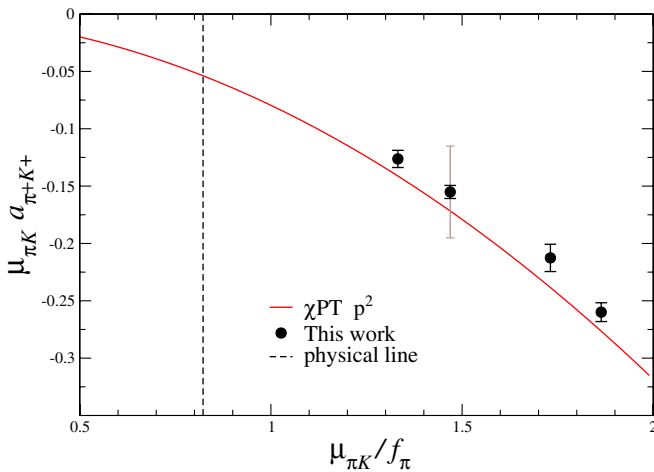


FIG. 2 (color online).  $\mu_{\pi K} a_{\pi^+ K^+}$  vs  $\mu_{\pi K}/f_\pi$ . The data points are the results of this lattice calculation, while the curve is the theoretical prediction at tree level in chiral perturbation theory [11]. The dark error bar is statistical, while the lighter error bar corresponds to the systematic error. The vertical dashed line denotes the physical pion and kaon masses.

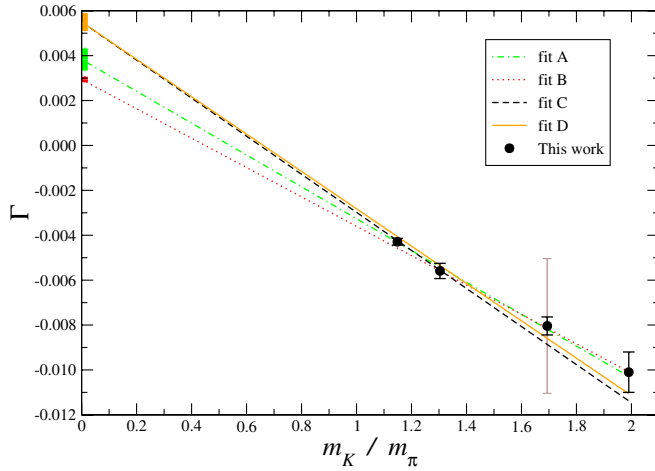


FIG. 3 (color online).  $\Gamma$  vs  $m_K/m_\pi$ . The dark error bar on the data points is statistical, while the lighter error bar corresponds to the systematic error. The lines correspond to the four linear fits (A,B,C,D). The bars on the y axis represent the  $1\text{-}\sigma$  errors in the determinations of  $L_5 = \Gamma(m_K/m_\pi = 0)$  as given in Table III. (At 95% confidence level, these determinations are in agreement.)

$L_5$  and  $L_{\pi K}$  (renormalized at  $f_\pi^{\text{phys}}$ ) can be determined.

Ideally, one would fit to lattice data at the lightest accessible values of the quark masses in order to ensure convergence of the chiral expansion. While we only have four different quark masses in our data set, with pion masses ranging from  $m_\pi \sim 290$  MeV to 600 MeV, fitting all four data sets and then “pruning” the heaviest data set and refitting provides a useful measure of the convergence of the chiral expansion. Hence, in “fit A”, we fit the data from all four lattice ensembles (m007, m010, m020 and m030), while in “fit B”, we fit the data from the lightest three lattice ensembles (m007, m010 and m020).

With the limited data set presently at our disposal, it is not practical to fit to the NNLO expression [10] for the scattering length. However, it is important to estimate the

uncertainty in the values of the scattering lengths extrapolated to the physical point that is introduced by the truncation of the chiral expansion at NLO. In our work on  $f_K/f_\pi$  [39] we extracted a value of  $L_5$  as it is the only NLO counterterm that contributes. The numerical value obtained is only perturbatively close to its true value, as it is contaminated by higher-order contributions. Therefore, by fixing the  $L_5$  that appears in Eq. (18) to the value of  $L_5$  extracted from  $f_K/f_\pi$ , an estimate of the uncertainty in both  $L_{\pi K}$  and in the extrapolated values of the scattering lengths due to the truncation of the chiral expansion can be estimated. Specifically, we sampled  $L_5$  from a Gaussian distribution for a range of  $f_K/f_\pi$  values [39] and then fit  $L_{\pi K}$  using  $\chi^2$ -minimization. We then generated a value of  $L_{\pi K}$  from a normal distribution formed from its mean and standard error. This fit is denoted “fit C”, and the same fit but with the m030 data pruned is denoted “fit D”. The results of the four fits are given in Table III and plotted in Fig. 3. These fits lead to an extraction of

$$L_{\pi K} = 4.16 \pm 0.18^{+0.26}_{-0.91}, \quad (19)$$

and a prediction of the scattering lengths extrapolated to the physical point of

$$\begin{aligned} m_\pi a_{3/2} &= -0.0574 \pm 0.0016^{+0.0024}_{-0.0058} \\ m_\pi a_{1/2} &= 0.1725 \pm 0.0017^{+0.0023}_{-0.0156}. \end{aligned} \quad (20)$$

We have chosen to take the central values and statistical errors from fit D and have set the systematic error due to truncation of the chiral expansion by taking the range of the various quantities allowed by the four fits, including statistical and systematic errors. In Fig. 4 we plot the 68% and 95% confidence-level error ellipses for the four fits given in Table III in the  $L_5$ - $L_{\pi K}$  plane. In Fig. 5 we plot the 95% confidence-level error ellipses associated with the four fits in the  $m_\pi a_{1/2}$ - $m_\pi a_{3/2}$  plane.<sup>4</sup> For purposes of comparison we have included the current-algebra point [11] on the plot as well as  $1\text{-}\sigma$  error ellipses from analyses

TABLE III. Results of the NLO fits. The values of  $m_\pi a_{3/2}$  and  $m_\pi a_{1/2}$  correspond to their extrapolated values at the physical point, where the error ellipses in the  $L_5$ - $L_{\pi K}$  plane have been explored at 68% confidence level (see Fig. 4).

FIT	$L_5 \times 10^3$	$L_{\pi K} \times 10^3$	$m_\pi a_{3/2}$	$m_\pi a_{1/2}$	$\chi^2/\text{dof}$
A	$3.83 \pm 0.49$	$3.55 \pm 0.20$	$-0.0607 \pm 0.0025$	$0.1631 \pm 0.0062$	0.17
B	$2.94 \pm 0.07$	$3.27 \pm 0.02$	$-0.0620 \pm 0.0004$	$0.1585 \pm 0.0011$	0.001
C	$5.65 \pm 0.02^{+0.18}_{-0.54}$ <sup>a</sup>	$4.24 \pm 0.17$	$-0.0567 \pm 0.0017$	$0.1731 \pm 0.0017$	0.84
D	$5.65 \pm 0.02^{+0.18a}_{-0.54}$ <sup>a</sup>	$4.16 \pm 0.18$	$-0.0574 \pm 0.0016$	$0.1725 \pm 0.0017$	0.90

<sup>a</sup>Input from  $f_K/f_\pi$  [39].

<sup>4</sup>In Mathematica format, the 95% confidence-level error ellipses in the  $m_\pi a_{1/2}$ - $m_\pi a_{3/2}$  plane are:

fit A: Ellipsoid [{0.1631, -0.0607}, {0.0197, 0.0007}, {{0.9283, 0.3719}, {-0.3719, 0.9283}}]  
 fit B: Ellipsoid [{0.1585, -0.0620}, {0.0076, 0.0004}, {{0.9461, 0.3239}, {-0.3239, 0.9461}}]  
 fit C: Ellipsoid [{0.1731, -0.0567}, {0.0042, 0.0016}, {{0.7534, 0.6576}, {-0.6576, 0.7534}}]  
 fit D: Ellipsoid [{0.1725, -0.0574}, {0.0046, 0.0027}, {{0.7881, 0.6156}, {-0.6156, 0.7881}}].

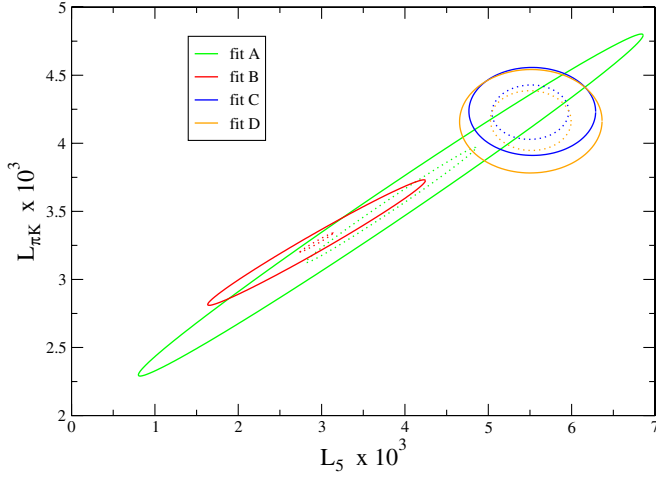


FIG. 4 (color online). Error ellipses in the  $L_5$ - $L_{\pi K}$  plane for the four fits (A,B,C,D) at 68% (dotted lines) and 95% (solid lines) confidence level.

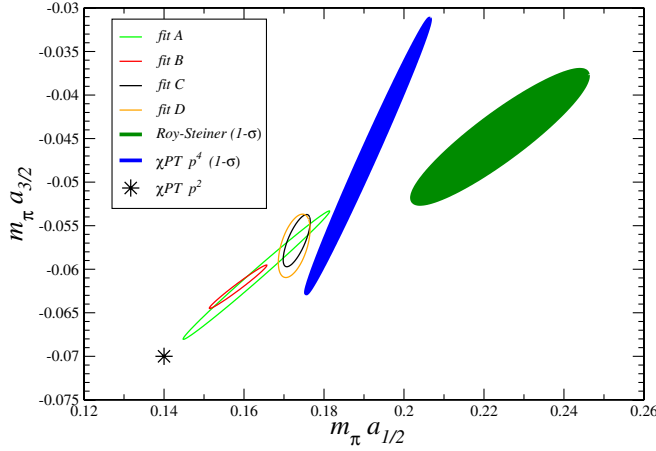


FIG. 5 (color online). Error ellipses for the four fits (A,B,C,D) at 95% confidence level. (Note that these results are derived from lattice data on a single lattice spacing of  $b = 0.125$  fm). The star corresponds to the current-algebra predictions ( $\chi\text{PT } p^2$ ) from Ref. [11]. We also display  $1-\sigma$  error ellipses from a  $\chi\text{PT}$  analysis at NLO [7] (denoted  $\chi\text{PT } p^4$ ) and from a fit using the Roy-Steiner equations [5].

based on fitting experimental data using  $\chi\text{PT}$  at NLO [7] and using Roy-Steiner equations [5]. As  $1-\sigma$  error ellipses correspond to 39% confidence level, one should be careful in finding discrepancy between the various determinations of the scattering lengths. It would be interesting to see the

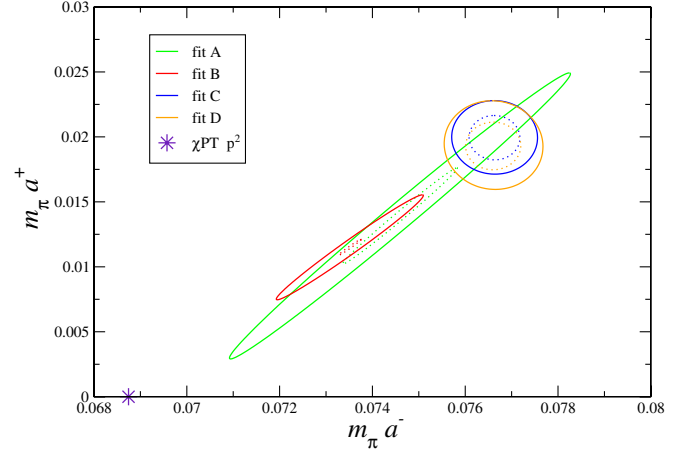


FIG. 6 (color online). Error ellipses for the four fits (A,B,C,D) at 68% (dotted lines) and 95% (solid lines) confidence level. The star corresponds to the current-algebra predictions ( $\chi\text{PT } p^2$ ) from Ref. [11].

NLO  $\chi\text{PT}$  and Roy-Steiner error ellipses at higher confidence levels.

For the sake of completeness, we also quote numbers for the crossing odd ( $a^-$ ) and crossing even ( $a^+$ ) scattering lengths extrapolated to the physical point:

$$\begin{aligned} m_\pi a^- &= 0.0766 \pm 0.0005^{+0.0000}_{-0.0032} \\ m_\pi a^+ &= 0.0193 \pm 0.0016^{+0.0021}_{-0.0080}, \end{aligned} \quad (21)$$

where the procedure for choosing the central value and determining the systematic error is the same as above. Error ellipses at 68% and 95% confidence levels are shown in Fig. 6.<sup>5</sup> The crossing-odd scattering length is of special interest as its corrections are protected by SU(2) chiral symmetry and are therefore of order  $m_\pi^4$  and expected to be small [40,41].<sup>6</sup>

Given how well our lattice data fit the NLO continuum  $\chi\text{PT}$  formulas, it would seem that the  $O(b^2)$  discretization errors are comparable or smaller than the systematic error due to omitted  $O(m_q^3)$  effects in the chiral expansion. However, one should keep in mind that our determinations of, for instance, the low-energy constants  $L_5$  and  $L_{\pi K}$  are subject to  $O(b^2)$  shifts. In contrast with the  $\pi^+\pi^+$  and  $K^+K^+$  scattering lengths, the mixed-action quantity  $\Delta_{\text{Mix}}$  makes an explicit contribution to the  $K^+\pi^+$  scattering length [42,43]. While this adds an additional unknown contribution to this process, a mixed-action  $\chi\text{PT}$  analysis

<sup>5</sup>In Mathematica format, the 95% confidence-level error ellipses in the  $m_\pi a^-$ - $m_\pi a^+$  plane are:  
 fit A: Ellipsoid  $\{[0.0746, 0.0139], [0.0116, 0.0004], \{[0.3150, 0.9491], [0.9491, -0.3150]\}\}$   
 fit B: Ellipsoid  $\{[0.0735, 0.0115], [0.0043, 0.0002], \{[0.3620, 0.9322], [0.9322, -0.3620]\}\}$   
 fit C: Ellipsoid  $\{[0.0766, 0.0200], [0.0029, 0.0009], \{[0.0014, 1.0000], [1.0000, -0.0014]\}\}$   
 fit D: Ellipsoid  $\{[0.0766, 0.0193], [0.0033, 0.0011], \{[-0.0017, 1.0000], [1.0000, 0.0017]\}\}$ .

<sup>6</sup>We thank Heiri Leutwyler for emphasizing this point to us.

of  $\pi K$  scattering, including lattice data from the fine MILC lattices ( $b \sim 0.09$  fm), will be able to address this source of systematic error quantitatively. We continue to search for the computational resources to accomplish this task.

## V. CONCLUSIONS

In this paper we have computed the  $\pi^+ K^+$  scattering length in fully-dynamical lattice QCD at pion masses ranging between  $m_\pi \sim 290$  MeV and 600 MeV. We have used the continuum expressions for the scattering lengths in SU(3) chiral perturbation theory, together with lattice data for  $f_K/f_\pi$ , to predict the physical  $I = 3/2$  and  $I = 1/2$   $\pi K$  scattering lengths with unprecedented accuracy. Naively one would expect that  $\pi^+ K^+$  scattering would give information about  $I = 3/2$  scattering only. However, the lattice data, when combined with chiral perturbation theory, implies a constraint on  $I = 1/2$  scattering as well. We anticipate that with improved statistics, together with calculations on lattices with smaller lattice spacings, the theoretically-predicted regions for  $m_\pi a_{3/2}$  and  $m_\pi a_{1/2}$  can be further reduced beyond those shown in Fig. 5. These regions can then be compared with the expected measurements from  $K^+ \pi^-$  atoms, to provide an exciting test of hadronic theory.

## ACKNOWLEDGMENTS

We thank Andre Walker-Loud and Donal O'Connell for useful conversations/correspondence and R. Edwards for help with the QDP++/Chroma programming environment [34] with which the calculations discussed here were performed. The computations for this work were performed at Jefferson Lab (JLab), Fermilab and Lawrence Livermore National Laboratory. We are indebted to the MILC and the LHP collaborations for use of their configurations and propagators, respectively. The work of M. J. S. was supported in part by the U.S. Department of Energy under Grant No. DE-FG03-97ER4014. The work of K. O. was supported in part by the U.S. Department of Energy contract No. DE-AC05-06OR23177 (JSA) and contract No. DE-AC05-84150 (SURA). The work of P.F.B. was supported in part by the U.S. Department of Energy grant No. ER-40762-365. The work of S.R.B. was supported in part by the National Science Foundation under grant No. PHY-0400231. Part of this work was performed under the auspices of the US DOE by the University of California, Lawrence Livermore National Laboratory under Contract No. W-7405-Eng-48. A.P. is supported by the Ministerio de Educación y Ciencia (Spain) under contract No. FIS2005-03142 and by the Generalitat de Catalunya under contract No. 2005SGR-00343.

- 
- [1] B. Adeva *et al.* (DIRAC Collaboration), Phys. Lett. B **619**, 50 (2005).
  - [2] S.R. Beane, P.F. Bedaque, K. Orginos, and M.J. Savage (NPLQCD Collaboration), Phys. Rev. D **73**, 054503 (2006).
  - [3] I. Caprini, G. Colangelo, and H. Leutwyler, Int. J. Mod. Phys. A **21**, 954 (2006).
  - [4] <http://dirac.web.cern.ch/DIRAC/future.html>.
  - [5] P. Buettiker, S. Descotes-Genon, and B. Moussallam, Eur. Phys. J. C **33**, 409 (2004).
  - [6] M. Jamin, J. A. Oller, and A. Pich, Nucl. Phys. **B587**, 331 (2000).
  - [7] V. Bernard, N. Kaiser, and U.G. Meissner, Nucl. Phys. **B357**, 129 (1991).
  - [8] V. Bernard, N. Kaiser, and U.G. Meissner, Phys. Rev. D **43**, R2757 (1991).
  - [9] B. Kubis and U. G. Meissner, Phys. Lett. B **529**, 69 (2002).
  - [10] J. Bijnens, P. Dhonte, and P. Talavera, J. High Energy Phys. 05 (2004) 036.
  - [11] S. Weinberg, Phys. Rev. Lett. **17**, 616 (1966).
  - [12] C. Miao, X. i. Du, G. w. Meng, and C. Liu, Phys. Lett. B **595**, 400 (2004).
  - [13] I. Caprini, G. Colangelo, and H. Leutwyler, Phys. Rev. Lett. **96**, 132001 (2006).
  - [14] S. Descotes-Genon and B. Moussallam, hep-ph/0607133.
  - [15] K. Huang and C.N. Yang, Phys. Rev. **105**, 767 (1957); H. W. Hamber, E. Marinari, G. Parisi, and C. Rebbi, Nucl. Phys. **B225**, 475 (1983); M. Lüscher, Commun. Math. Phys. **105**, 153 (1986); Nucl. Phys. **B354**, 531 (1991).
  - [16] S.R. Beane, P.F. Bedaque, A. Parreño, and M.J. Savage, Phys. Lett. B **585**, 106 (2004).
  - [17] D.B. Renner *et al.* (LHP Collaboration), Nucl. Phys. B, Proc. Suppl. **140**, 255 (2005).
  - [18] R.G. Edwards *et al.* (LHPC Collaboration), PoS, LAT2005 (2006) 056.
  - [19] K. Orginos, D. Toussaint, and R.L. Sugar (MILC Collaboration), Phys. Rev. D **60**, 054503 (1999).
  - [20] K. Orginos and D. Toussaint (MILC collaboration), Phys. Rev. D **59**, 014501 (1998).
  - [21] S. Durr and C. Hoelbling, Phys. Rev. D **71**, 054501 (2005).
  - [22] C. Bernard, Phys. Rev. D **73**, 114503 (2006).
  - [23] M. Creutz, hep-lat/0603020.
  - [24] C. Bernard, M. Golterman, Y. Shamir, and S.R. Sharpe, hep-lat/0603027.
  - [25] S. Durr and C. Hoelbling, Phys. Rev. D **74**, 014513 (2006).
  - [26] A. Hasenfratz and R. Hoffmann, Phys. Rev. D **74**, 014511 (2006).
  - [27] C. Bernard, M. Golterman, and Y. Shamir, Phys. Rev. D **73**, 114511 (2006).
  - [28] Y. Shamir, hep-lat/0607007.
  - [29] C.W. Bernard *et al.*, Phys. Rev. D **64**, 054506 (2001).
  - [30] A. Hasenfratz and F. Knechtli, Phys. Rev. D **64**, 034504 (2001).

- [31] T.A. DeGrand, A. Hasenfratz, and T.G. Kovacs, Phys. Rev. D **67**, 054501 (2003).
- [32] T.A. DeGrand (MILC Collaboration), Phys. Rev. D **69**, 014504 (2004).
- [33] S. Durr, C. Hoelbling, and U. Wenger, Phys. Rev. D **70**, 094502 (2004).
- [34] R. G. Edwards and B. Joo (SciDAC Collaboration), Nucl. Phys. B, Proc. Suppl. **140**, 832 (2005).
- [35] C. McClendon, Jlab Report No. JLAB-THY-01-29, 2001 (unpublished).
- [36] J. Gasser and H. Leutwyler, Nucl. Phys. **B250**, 465 (1985).
- [37] J. Gasser and H. Leutwyler, Ann. Phys. (N.Y.) **158**, 142 (1984).
- [38] J. Gasser and H. Leutwyler, Phys. Lett. B **125**, 321 (1983).
- [39] S.R. Beane, P.F. Bedaque, K. Orginos, and M.J. Savage, hep-lat/0606023.
- [40] A. Roessl, Nucl. Phys. **B555**, 507 (1999).
- [41] J. Schweizer, Phys. Lett. B **625**, 217 (2005).
- [42] J.W. Chen, D. O'Connell, R.S. Van de Water, and A. Walker-Loud, Phys. Rev. D **73**, 074510 (2006); (to be published).
- [43] D. O'Connell, "Ginsparg-Wilson Meson Scattering on a Staggered Sea," talk at LATTICE 2006, Tucson, Arizona.